

## Highly Selective Behavior of Thin Film ZnO Based Homojunction Photodetector for UV Sensing

Lucky Agarwal<sup>1</sup>, K. Sambasiva Rao<sup>2</sup>, Ravi Prakash Dwivedi<sup>1,\*</sup>

<sup>1</sup> School of Electronics Engineering, Vellore Institute of Technology, 600127 Chennai, India

<sup>2</sup> Department of Electronics & Communication Engineering, Hindustan Institute of Technology, 600126 Chennai, India

(Received 12 February 2022; revised manuscript received 18 April 2022; published online 29 April 2022)

ZnO is considered as a prominent semiconductor material in the II-VI metal-oxide group due to its exceptional optical properties that persuade many researchers to use it in the fabrication of photodetectors for ultraviolet (UV) sensing applications. The sensitivity of a photodetector is measured in terms of its responsivity. In this article, the authors have reported a *p-n* homojunction based on nanostructured ZnO thin film for application as a photodetector in the UV region. The *p*-type nature of ZnO was obtained by selective doping of ZnO with copper. Hall and hot point probe measurements confirmed that the deposited Cu doped ZnO (CZO) thin film poses *p*-type conductivity with a resistivity of 0.9  $\Omega$ -cm, carrier concentration of  $1.0287 \times 10^{18} \text{ cm}^{-3}$  and mobility of 6.5  $\text{cm}^2/\text{Vs}$  at room temperature. The crystalline, morphological studies of ZnO films have been performed by X-ray diffractometer (XRD), atomic force microscopy (AFM), energy dispersive spectrum (EDAX). The current-voltage (*I-V*) measurements under dark and illuminated conditions have been carried out using Semiconductor Device Analyzer (SDA). The fabricated device shows good rectification property with low reverse leakage current and high rectification ratio. The device has been found to be stable and exhibiting a high value of responsivity (3.2 A/W) at 376 nm for a reverse bias voltage of 3 V. The performance of the new *p-n* junction ZnO based UV detector is found to outstrip the existing ZnO based Schottky diode photodetectors.

**Keywords:** CZO, Homojunction, Photodiode, Responsivity, Thin film, ZnO.

DOI: [10.21272/jnep.14\(2\).02009](https://doi.org/10.21272/jnep.14(2).02009)

PACS numbers: 42.79.Pw, 85.60.Gz

### 1. INTRODUCTION

Photonics has been hailed as the technology of promise for generating and harnessing light. In reality, progress towards a photonic driven circuit is disturbed by the downscaling of optoelectronic components. The present developing one of the fields of optoelectronics is known as photodetector. Over the last few decades research has been motivated towards the fabrication of a multilayer substrate with good interconnectivity in the field of detectors. The optosensing field must have the potential to advance existing structure along with sagacious future innovation system. These days, application of *p-n* junction as a photodetector goes through a broad selection of wavelength range, including X-rays, infrared, and ultraviolet (UV) [1]. Conventional photodetectors are used to sense a selected wavelength region and to turn into blind in the rest of the regions. Exposure of UV radiation for making photodetectors is found suitable for several non-telecommunication applications, involving missile warning systems, furnace control, aerospace, flame detection, biomedical applications, and also space to space communication [2-5]. Consequently, there is a scope for the development of different photodiodes for UV sensing applications. Several researchers have developed UV detectors based on thin film heterojunctions [6-8]. Oxide semiconductors are becoming attractive for the development of a variety of thin film based devices for UV sensing applications [9].

Among various oxide semiconductors, ZnO has been studied extensively by the researchers in view of several interesting properties of the material such as high

exciton energy ( $\sim 60$  meV) and a large band gap with low-cost manufacturing.

A large number of ZnO thin-film and nanostructure-based devices have been reported in the literature for a variety of electronic and optoelectronic applications [10-12]. One of the major areas of ZnO based devices is photodetection in the UV region. Most of the ZnO based devices uses either a Schottky junction or a heterojunction for photodetection applications. This is because ZnO has inherent *n*-type conductivity, and it is extremely difficult to produce high quality and stable *p*-type ZnO films (due to the presence of defects) [13, 14]. In view of the complication coupled with the attainment of *p*-nature in ZnO with high stability, numerous ZnO based *p-n* heterojunction and Schottky junction photodetectors have been reported in the literature [15, 16]. In this context, Chen et al. [15] reported the ZnO based photodetector with  $\text{IrO}_2$  as Schottky contact on ZnO thin film. The photocurrent was observed to be 2 orders higher than the dark current. The reported responsivity is 0.011 A/W at 360 nm for a bias of 5 V. Ali et al. [16] reported the Au/Cr Schottky junction UV photodetectors, using ZnO thin film deposited by sol-gel spin coating method. The maximum responsivity reported for the proposed metal semiconductor metal (MSM) structure was 0.056 A/W. Further, Lin et al. [17] fabricated the Schottky junction between Ruthenium (Ru) and ZnO films. The reported responsivity was found to be 0.01 A/W. The reported responsivity of UV photodetectors based on ZnO Schottky contacts is observed to be poor because of the large barrier height at the metal semiconductor junction [18].

\* [raviecit@gmail.com](mailto:raviecit@gmail.com)

It is clear from the literature that the use of  $p$ - $n$  heterojunctions can improve the responsivity of a photodetector at the cost of speed of response. In this connection, Rana et al. [19] investigated the effect of UV light on the  $p$ -NiO/ $n$ -ZnO structure and the measured responsivity was 0.29 A/W at 365 nm. Zhang et al. [20] observed a UV photoresponse on GaN/ZnO nanorods  $p$ - $n$  heterojunction structure. The peak response of 138.9 mA/W was observed at 362 nm. Although some advantages such as low dark current and improved responsivity were observed in ZnO heterojunction photodetectors, the peak responsivity is still much lower. Further, the  $n$ -ZnO/ $p$ -Si heterojunction photodetectors reported by Chen et al. [21] showed a photoresponse in the UV and visible regions due to the large difference in the band gap of ZnO and Si. The difference in the band gap creates a discontinuity at the junction, which limits its application in UV detection. Therefore, to achieve a high photoresponse in the UV region, study of a new junction structure is essential which can overcome the large barrier height of Schottky junction and band discontinuity of heterojunction.

Based on the literature, it is observed that the use of a conventional  $p$ - $n$  junction can significantly improve the responsivity of a photodetector [22]. In this paper, a new approach was proposed for the fabrication of a stable ZnO based  $p$ - $n$  homojunction UV photodetector on ITO coated glass. The junction was formed between RF sputter deposited  $n$ -type ZnO thin film and sol gel spin coated  $p$ -type ZnO thin film. The  $p$ -type nature in ZnO was obtained by selective doping of copper in ZnO [23]. Further, simulations were carried out by using SILVACO Atlas™ to validate the experimental results. The surface morphological study of the CZO and ZnO thin films was performed by atomic force microscopy (AFM), while the structural study was carried out using X-ray diffraction. The type of conductivity of the deposited films was also determined using Hall measurement set-up. The electrical properties of the proposed detector such as barrier height, ideality factor, responsivity, were evaluated by using a semiconductor parameter analyzer.

## 2. FABRICATION STEPS OF THE PROPOSED PHOTODETECTOR

The proposed photodetector is a homojunction between ZnO and CZO (copper doped ZnO). For this, initially ZnO thin film with a thickness of about 300 nm was deposited by RF sputtering method on the ITO coated glass substrate. Afterwards, the deposited sample was annealed in argon ambient to form nanostructures. The nanostructures increase the transmittance property of thin films. Further, to form a junction, the 5 mol % CZO sol was prepared using zinc acetate dehydrate, isopropanol, diethanolamine and copper acetate dehydrate. After aging, the prepared sol was spin coated on the grown ZnO nanostructured thin film. To reach the desired thickness of CZO thin film, the coating process was repeated sequentially for five times. Afterwards, the deposited film was annealed at 500 °C in a muffle furnace for 1 h. The 5 mol % CZO layer was chosen, since it shows stable  $p$ -type conductivity with a high hole concentration of  $1.0217 \times 10^{18}$  per  $\text{cm}^3$ , and

mobility of  $6.5 \text{ cm}^2/\text{V}\cdot\text{s}$ . The elemental and weight composition of CZO thin film was studied by energy dispersive analysis (EDAX). Fig. 1 shows the EDAX spectrum of the deposited CZO thin film on undoped ZnO. Table 1 shows the elemental composition of CZO. EDX analysis confirms the presence of copper in the ZnO lattice.

Afterwards, the top metal contacts of the  $p$ - $n$  homojunction were engineered. To accomplish this, aluminum metal dots were fledged over the ZnO layer by the thermal deposition method. The area of the deposited contact is  $0.25 \text{ cm}^2$ . The aluminum dots form an ohmic contact with ZnO thin film; simultaneously ITO forms an ohmic contact with CZO thin film. The resultant structure is termed as a diode. The schematic of the CZO/ZnO diode is shown in Fig. 2.

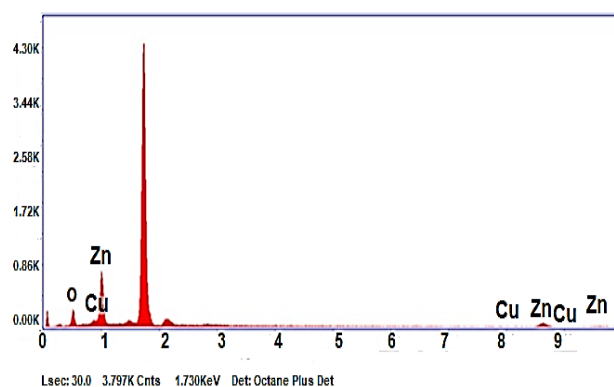


Fig. 1 – Energy dispersive spectrum of CZO thin film

Table 1 – Elemental composition

Element	Weight %
O K	15.68
Cu L	5.77
Zn L	78.55

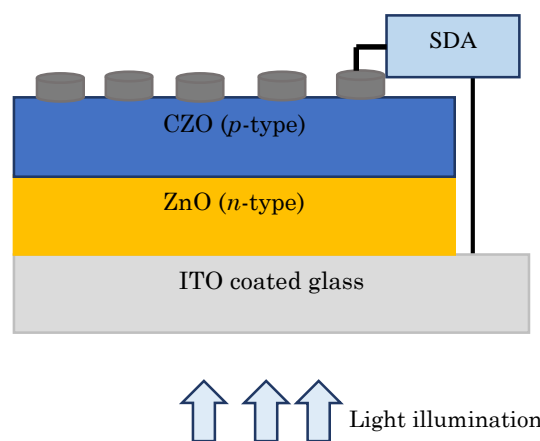


Fig. 2 – Schematic of the fabricated  $p$ - $n$  homojunction device

## 3. RESULTS AND DISCUSSION

### 3.1 Structural Analysis of Nanocrystalline Films

X-ray diffraction (XRD) patterns of ZnO and CZO thin films are shown in Fig. 3. XRD peaks of the deposited films show the same pattern as reported for ZnO wurtzite structure (JCPDS, 36-1451) [24]. The deposited films exhibit a hexagonal wurtzite structure with a

preferred (101) orientation. XRD spectrum peak intensity also shows that the incorporation of copper into the ZnO lattice increases the grain growth rate. The equivalent crystal size and lattice constants of the deposited thin films were extracted from the XRD pattern and are listed in Table 2. It is observed from Table 2 that there is a slight decrease in the grain size of CZO thin film due to the presence of Cu atoms in Zn interstitial sites which decreases the nucleation points and hence reduces the crystal size [13]. Further, the thickness of the deposited thin films was evaluated from the ellipsometer, and the results are given in Table 2. Fig. 4 shows the AFM images of the deposited ZnO thin film on ITO coated glass substrate and CZO thin film on ZnO, respectively. It can be seen from Fig. 4a that a uniform nanostructure has been grown on ITO coated glass. The grain size of the nanostructured thin film is the same as the grain size calculated from the XRD results. Further, the roughness profile was analyzed and calculated whose value is 3.43 nm. This low roughness value suggests that the deposited film is uniform, which confirms the high transmittivity of undoped ZnO thin film [25].

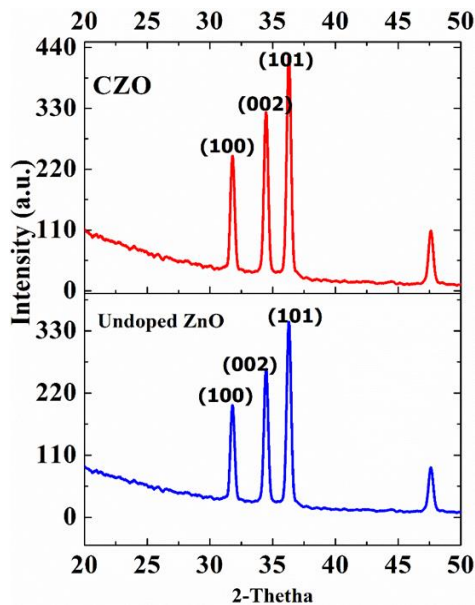


Fig. 3 – XRD spectrum of undoped and CZO thin films

Table 2 – Structural parameters evaluated from XRD results

Sample	Film thickness (nm)	Lattice constant <i>a</i> (Å)	Lattice constant <i>c</i> (Å)	Crystal size (nm)
Values (JPCDS card no: 36-1451)		3.25	5.207	
ZnO	220	3.253	5.206	52
CZO	198	3.256	5.198	36

Fig. 4b shows the AFM image of the CZO thin film. As can be seen from Fig. 4b, many large voids formed which may be due to the incorporation of Cu ions into ZnO interstitials [13]. This leads to a reduction in the crystal size, which reduces optical scattering, thereby resulting in high optical reflectivity. High reflectivity is desired from the top surface of the photodetector to confine the light within the junction.

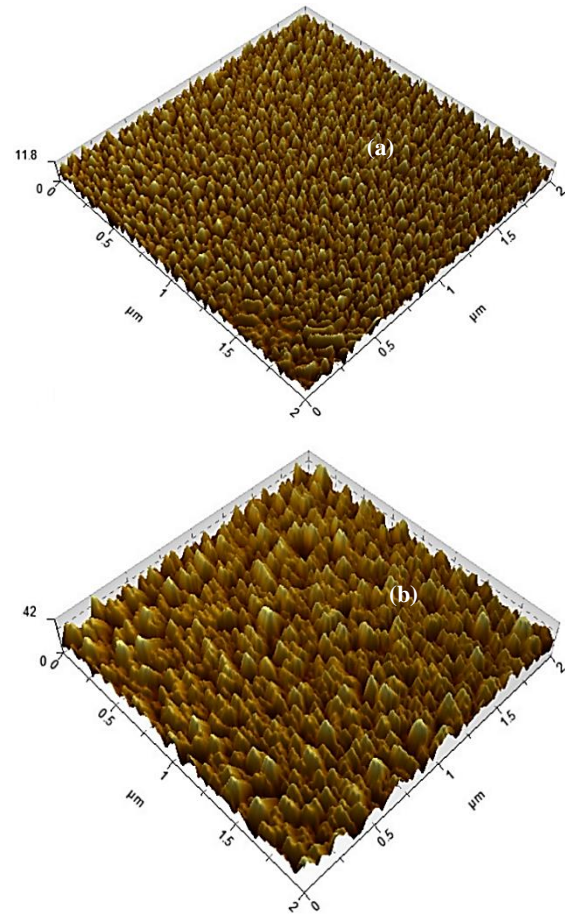


Fig. 4 – AFM images of (a) undoped ZnO thin film, (b) CZO thin film

### 3.2 Electrical Characterization of Deposited Thin Films

#### a. Hall Effect and Hot Point Probe Measurement

Hall-effect measurements and hot point measurements have been done in order to obtain the conductivity of the deposited thin films. Hall measurements have been done at room temperature in vacuum to calculate the conductivity, mobility and carrier concentration of the deposited thin films. The obtained data from the measurements is listed in Table 3, which shows that the undoped film shows *n*-type conductivity, while CZO film shows *p*-type conductivity. To validate the results obtained from the Hall measurements, hot point probe measurements based on the Seebeck effect have been carried out with the help of a voltmeter and soldering iron. The calculated negative Seebeck coefficient of 550  $\mu\text{V/K}$  confirms the *p*-type nature of CZO thin film.

Table 3 – Electrical parameters evaluated from the Hall measurements

Sample	Carrier concentration ( $\text{cm}^{-3}$ )	Mobility ( $\text{cm}^2/\text{V}\cdot\text{s}$ )	Conduction type
ZnO	$2.0954 \times 10^{21}$	25.5	<i>n</i>
CZO	$1.0217 \times 10^{18}$	6.5	<i>p</i>

### b. *I-V* Measurement

The current-voltage (*I-V*) characteristics of the fabricated *p-n* homojunction device structure (as shown in Fig. 2) have been obtained from the semiconductor device analyzer (SDA). Fig. 5 illustrates the *I-V* characteristics of the fabricated ZnO *p-n* homojunction under dark conditions and UV illumination. From Fig. 5, it is observed that under dark conditions, the current increases nonlinearly with the forward bias and negligible amount of current during reverse bias which shows the rectifying behavior of a typical *p-n* junction device.

**Table 4** – Electrical parameters of the fabricated photodetector

Parameters	Cut-in potential	Rectification ratio	Reverse saturation current
Under dark condition	1.12 V	10012	3.2 nA
Under UV illumination	0.98 V	10	0.6 $\mu$ A

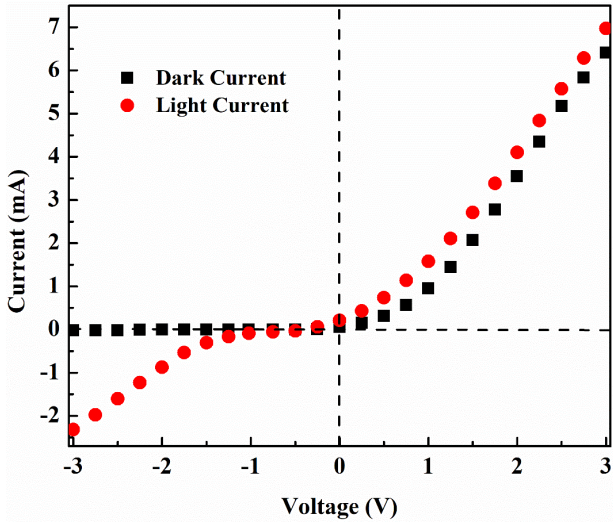


**Fig. 5** – *I-V* characteristics of the fabricated *p-n* homojunction photodetector

This increase is usual for wide band gap *p-n* homojunction due to the recombination-tunneling mechanism [17]. The fabricated photodetector shows a forward current of 7 mA under UV illumination and  $\sim 6.4$  mA under dark conditions at a bias voltage of 3 V. The reverse current increases from 0.05  $\mu$ A in the dark to 2.5 mA under UV illumination at a reverse bias voltage of  $-3$  V. The increase in reverse current is due to the generation of excess charge carriers because of incident photons. To verify the stability and consistency of the result, the authors made 20 devices, and 95 % of them showed good rectifying behavior. The behavior of all devices remained the same even after they were exposed to the atmosphere for more than 450 days.

The diode ideality factor was evaluated from the diode current equation as given below:

$$I = I_0 \left( e^{\frac{qV}{\eta kT}} - 1 \right), \quad (1)$$

where  $k$  is the Boltzmann constant, and  $T$  is the absolute temperature,  $\eta$  is the ideality factor,  $I_0$  is the re-

verse saturation current at  $V=0$ . The ideality factor derived from Eq. (1) is 3.1. It is higher than for ideal *p-n* junction device. A higher ideality factor suggests that there are multiple current transport mechanisms at the junction, such as carrier recombination in the space-charge region, deep-level-assisted tunneling and parasitic rectification within the device [26]. The other evaluated electrical parameters from the fabricated photodetector are indexed in Table 4.

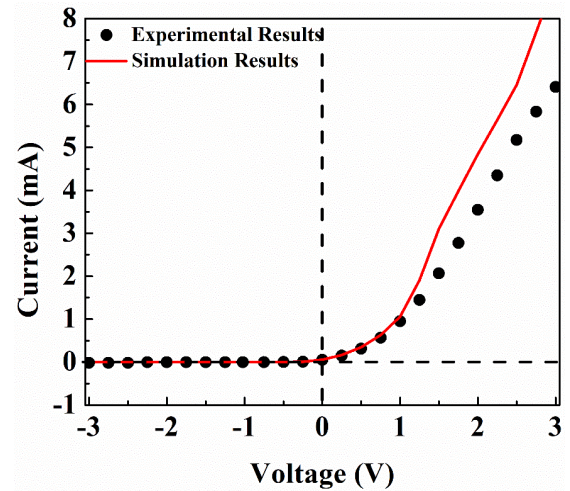
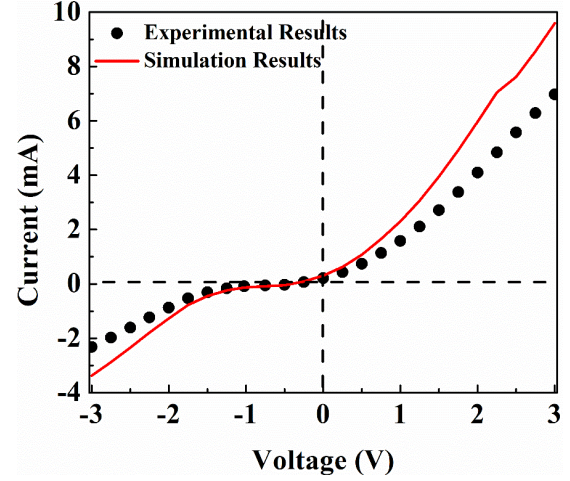


**Fig. 6** – Simulated and experimental *I-V* characteristics of the photodetector under (a) UV illumination, (b) dark conditions

To simulate the proposed photodetector structure and validate the experimental results, two-dimensional (2D) simulations were carried out using standard commercial software SILVACO Atlas. The simulated results were plotted by using Tonyplot. The *I-V* characteristics of the simulated device were obtained by solving 2D Poisson and Laplace equations. Auger model was incorporated during simulation for carrier generation and recombination. Further, a field-dependent mobility model was used to evaluate the charge circulation in the proposed structure. To incorporate the light beam illumination on the photodetector, the optical model of the light beam was also incorporated in the simulation. ZnO and CZO materials were not available in the Atlas library, hence a library was created for ZnO and CZO. The variation of the *I-V* characteristic under UV illumination and dark conditions are plotted

in Fig. 6a and Fig. 6b, respectively. It can be observed that the simulated results followed the same trend as experimental data. Hence, further studies were carried out to observe the optical characteristics of the proposed device.

### 3.3 Photoresponse

An ITO coated glass substrate was used as a “low pass filter” which absorbs light below wavelength of 320 nm [22]. Therefore, light passes through the glass side of the fabricated device to transmit a higher order wavelength at the junction. Further, the absorption spectrum was plotted (using ellipsometer) to visualize the absorption region of the device shown in Fig. 7. An absorption peak is observed at a wavelength of 376 nm. This wavelength corresponds to the band gap of ZnO. From the results, it can be inferred that by varying the doping element, it is possible to adjust the band gap of the device, and therefore selective photodetectors within the specified range.

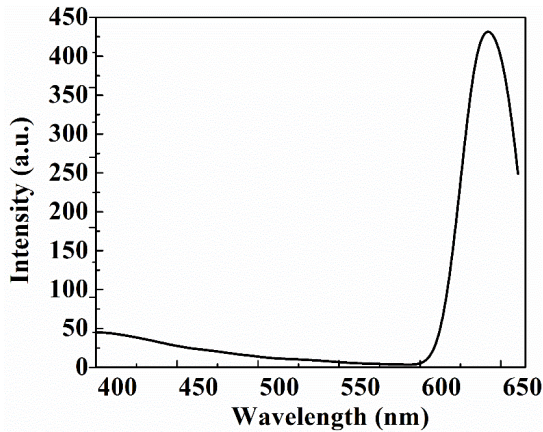


Fig. 7 – Absorbance characteristics of the fabricated photodetector

Fig. 8 depicts the photoresponse characteristic of the fabricated homojunction photodetector at a reverse bias of 3 V. As the responsivity is measured at a specific wavelength, a diffraction grating monochromator is used which selects a narrow wavelength from a broad band lamp source such as a tungsten lamp. The wavelength is tuned continuously in order to measure the responsivity of the photodetector. As can be observed from Fig. 8, the photoresponse of the device begins around 300 nm in the UV region and extends into the visible region. The responsivity increases steadily, reaching a peak around 376 nm which corresponds to the effective band gap of ZnO.

The responsivity increases from 0.6 A/W and reaches 3.2 A/W in the UV region and decreases for higher order wavelengths. Since ZnO shows the transparency of more than 90 % in the visible region, therefore, most of the photons will be absorbed by *p*-type CZO that generate EHPs. As evaluated from Fig. 5, a high potential barrier of 0.98 V is created at the *n*-ZnO/*p*-CZO interface.

When a reverse voltage is applied across the junction, the Fermi level of the *p*-CZO thin film rises to a

higher value, which leads to further expansion of the potential barrier across the interface. This in turn enhances the induced electric field across the space charge region that opens up a large number of available states for the holes to be injected into CZO. Under illumination, a decrease in the potential barrier gives rise to electron-hole pair generation that are finally separated by this increased electric field and hence a high responsivity is obtained. In addition, simulations were carried out to validate the experimental results. It can be observed from Fig. 8 that there is good agreement between experimental and simulation results.

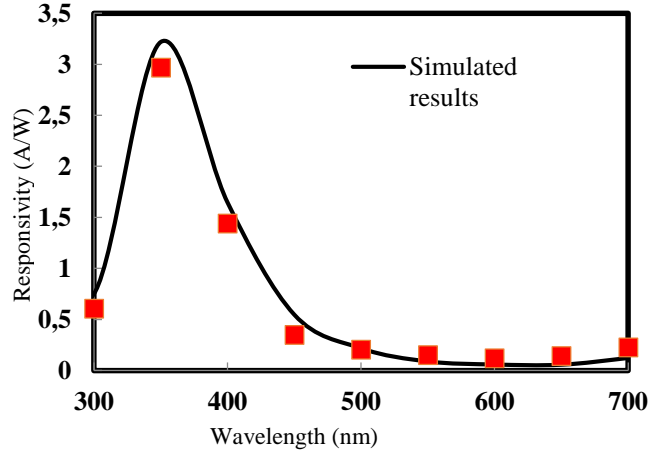


Fig. 8 – Photoresponse characteristic of the photodetector

The responsivity peak at 376 nm is not commonly observed in most ZnO-based photodetectors reported earlier [16, 18]. The occurrence of the peak may be due to two features of the device such as introduction of the *p*-ZnO layer and ITO/glass substrate. The ITO/glass substrate filters light with higher energy, while the ZnO layer absorbs light with energy close to its band gap. Further, the aforementioned photoresponse spectrum can be understood by studying the charge transport mechanism in homojunction structures.

The photoresponse of the fabricated photodetector can be further analyzed by measuring the specific detectivity (*D*) of the device. Specific detectivity is a Figure of Merit (FOM) for device application, whose large value certifies the photodetector for low noise applications. Mathematically it can be expressed as [26]:

$$D = R \left( \frac{R_0 A}{4kT} \right)^{0.5}, \quad (2)$$

where *R* is the responsivity, *R*<sub>0</sub>*A* is the zero-biased resistance area product of the device, which can be obtained from the *J*-*V* characteristics as:

$$R_0 A = \left( \frac{\partial J}{\partial V} \right)^{-1} = a \left( \frac{\partial I}{\partial V} \right)^{-1}. \quad (3)$$

The value of *R*<sub>0</sub>*A* product obtained from Fig. 5 is approximately 8.96 Ω·cm<sup>2</sup> at zero bias. The evaluated specific detectivity of the photodetector from Eq. (2) is 2.9 × 10<sup>9</sup> mHz<sup>1/2</sup>/W.

#### 4. CONCLUSIONS

A low-cost ZnO homojunction photodetector fabricated by sol-gel spin coating and RF sputtering method has been proposed in this paper. The forward cut-in voltage of the fabricated device is 0.98 V with a reverse leakage current of 3.2 nA and a rectification ratio of 10012. The fabricated device exhibits good rectification properties in the dark region. The proposed device can work as a UV photodetector when light passes through the glass side. The photodetector shows a forward current of 7 mA and a reverse current of 2.5 mA under UV illumination. The photodetector also shows an excellent responsivity of 3.2 A/W at a wavelength of 376 nm with a reverse bias of 3 V. Further, the detectivity of the

device was calculated, the value of which is equal to  $2.9 \times 10^9 \text{ mHz}^{1/2}\text{W}^{-1}$  at zero bias. This work suggests that an efficient UV photodetector can be fabricated based on ZnO homojunction with simple design steps. Finally, simulations were carried out whose results are in-line with the experimental results of the proposed device structure. This gives confidence that the proposed device can be used for commercial applications.

#### ACKNOWLEDGEMENTS

The authors gratefully acknowledge Advance Imaging Centre, IIT Kanpur and Centre for Interdisciplinary Research (CIR), MNNIT, Allahabad for providing characterization facilities.

#### REFERENCES

- G. Rawat, D. Somvanshi, H. Kumar, Y. Kumar, C. Kumar, S. Jit, *IEEE T. Nanotechnol.* **15** No 2, 193 (2015).
- Y. Kumar, H. Kumar, G. Rawat, C. Kumar, B.N. Pal, S. Jit, *IEEE Photon. Technol. Lett.* **30** No 12, 1147 (2018).
- M.A. Seyedi, M. Yao, J. O'brien, S. Wang, P.D. Dapkus, *Appl. Phys. Lett.* **103** No 25, 251109 (2013).
- L. Rajan, C. Periasamy, V. Sahula, *IEEE T. Nanotechnol.* **15** No 2, 201 (2016).
- L. Agarwal, S. Tripathi, *Semicond. Sci. Technol.* **35** No 6, 065001 (2020).
- D. Kumar, T. Gomes, N. Alves, J. Kettle, *IEEE Sensors* **1** (2018).
- Z. Bai, Z. Liu, *IEEE Sensors* **1** (2017).
- A. Kumar, D. Bose, *IETE J. Res.* **43** No 2-3, 257 (1997).
- L. Agarwal, B. Singh, S. Tripathi, P. Chakrabarti, *2017 Conference on Emerging Devices and Smart Systems (ICEDSS)*, 180 (2017).
- R. Chakraborty, U. Das, D. Mohanta, A. Choudhury, *Indian J. Phys.* **83** No 4, 553 (2009).
- N. Sharma, V. Puri, *IETE J. Res.* **1** (2020).
- J. Kar, S. Das, J. Choi, Y. Lee, T. Lee, J. Myoung, *J. Crystal Growth* **311** No 12, 3305 (2009).
- L. Agarwal, S. Tripathi, P. Chakrabarti, *Mater. Focus* **7** No 1, 18 (2018).
- G. Saxena, R. Paily, *IETE J. Res.* **66** No 4, 579 (2020).
- K.-J. Chen, F.-Y. Hung, S.-J. Chang, S.-J. Young, *J. Alloy. Compd.* **479** No 1-2, 674 (2009).
- G.M. Ali, P. Chakrabarti, *J. Phys. D: Appl. Phys.* **43** No 41, 415103 (2010).
- T. Lin, S.-J. Chang, Y.-K. Su, B. Huang, M. Fujita, Y. Horikoshi, *J. Crystal Growth* **281** No 2-4, 513 (2005).
- J.U. Lee, P. Gipp, C. Heller, *Appl. Phys. Lett.* **85** No 1, 145 (2004).
- A.K. Rana, M. Kumar, D.-K. Ban, C.-P. Wong, J. Yi, J. Kim, *Adv. Electron. Mater.* **5** No 8, 1900438 (2019).
- L. Zhang, F. Zhao, C. Wang, F. Wang, R. Huang, Q. Li, *Electron. Mater. Lett.* **11** No 4, 682 (2015).
- L.-C. Chen, C.-N. Pan, *Eur. Phys. J.: Appl. Phys.* **44** No 1, 43 (2008).
- Y.H. Leung, Z. He, L. Luo, C. Tsang, N. Wong, W. Zhang, S. Lee, *Appl. Phys. Lett.* **96** No 5, 053102 (2010).
- K. Tam, C. Cheung, Y. Leung, A. Djuri S'ic', C. Ling, C. Belling, S. Fung, W.M. Kwok, W. Chan, D. Phillips, et al., *J. Phys. Chem. B* **110** No 42, 865 (2006).
- G. Paul, S. Bandyopadhyay, S. Sen, S. Sen, *Mater. Chem. Phys.* **79** No 1, 71 (2003).
- J. Fedison, T. Chow, H. Lu, I. Bhat, *Appl. Phys. Lett.* **72**, No 22, 2841 (1998).
- A. Rajan, H.K. Yadav, V. Gupta, M. Tomar, *Procedia Engineering* **94**, 44 (2014).

### Високоселективна поведінка фотодетектора з гомопереходом на основі тонкоплівкового ZnO для УФ-зондування

Lucky Agarwal<sup>1</sup>, K. Sambasiva Rao<sup>2</sup>, Ravi Prakash Dwivedi<sup>1</sup>

<sup>1</sup> School of Electronics Engineering, Vellore Institute of Technology, 600127 Chennai, India

<sup>2</sup> Department of Electronics & Communication Engineering, Hindustan Institute of Technology, 600126 Chennai, India

ZnO вважається важливим напівпровідниковим матеріалом у II-VI групах метал оксидів завдяки винятковим оптичним властивостям, які переконують багатьох дослідників використовувати його у виготовленні фотодетекторів для ультрафіолетового (УФ) зондування. Чутливість фотодетектора вимірюється через його сприйнятливості. У статті автори повідомили про *p-n* гомоперехід на основі наноструктурованої тонкої плівки ZnO для застосування його як фотодетектора в УФ-області. ZnO *p*-типу був отриманий селективним легуванням ZnO міддю. Вимірювання Холла та зонда гарячої точки підтвердили, що осаджена тонка плівка ZnO (CZO), легована Cu, має провідність *p*-типу з питомим опором 0,9 Ом-см, концентрацією носіїв  $1,0287 \times 10^{18} \text{ см}^{-3}$  і рухливостю  $6,5 \text{ см}^2/\text{В-с}$  за кімнатної температури. Кристалічні морфологічні дослідження плівок ZnO проводили за допомогою рентгенівського дифрактометра (XRD), атомно-силової мікроскопії (AFM), енергодисперсійного спектру (EDAX). Вимірювання залежності струму від напруги (*I-V*) у темряві та при освітленні проводили з використанням аналізатора напівпровідникових пристроїв. Виготовлений пристрій має гарні властивості випрямлення із низьким зворотним струмом витоку та високим коефіцієнтом випрямлення. Виявилося,

що пристрій стабільний і демонструє високе значення сприйнятливості 3,2 А/Вт при 376 нм для напруги зворотного зміщення 3 В. Виявлено, що продуктивність нового УФ-детектора з *p-n* переходом на основі ZnO перевершує існуючі фотодетектори з діодами Шотткі на основі ZnO.

**Ключові слова:** CZO, Гомоперехід, Фотодіод, Чутливість, Тонка плівка, ZnO.